ME8H03

UNCLASSIFIED [redacted]

COPY NO. 133
RM No. E8H03

NACA

RESEARCH MEMORANDUM

COOLING OF GAS TURBINES

IX - COOLING EFFECTS FROM USE OF CERAMIC COATINGS ON WATER-COOLED TURBINE BLADES

By W. Byron Brown and John N. B. Livingood

Lewis Flight Propulsion Laboratory
Cleveland, Ohio

NATIONAL ADVISORY COMMITTEE FOR AERONAUTICS

WASHINGTON
October 13, 1948

[redacted]

UNCLASSIFIED

 [redacted]

NATIONAL ADVISORY COMMITTEE FOR AERONAUTICS

RESEARCH MEMORANDUM

COOLING OF GAS TURBINES

IX - COOLING EFFECTS FROM USE OF CERAMIC COATINGS ON WATER-COOLED TURBINE BLADES

By W. Byron Brown and John N. B. Livingood

SUMMARY

The hottest part of a turbine blade is likely to be the trailing portion. When the blades are cooled and when water is used as the coolant, the cooling passages are placed as close as possible to the trailing edge in order to cool this portion. In some cases, however, the trailing portion of the blade is so narrow, for aerodynamic reasons, that water passages cannot be located very near the trailing edge. Because ceramic coatings offer the possibility of protection for the trailing part of such narrow blades, a theoretical study has been made of the cooling effects of such coatings. This study calculates the effect of a ceramic coating on: (1) the blade-metal temperature when the gas temperature is unchanged, and (2) the gas temperature when the metal temperature is unchanged. Comparison is also made between the changes in the blade or gas temperatures produced by ceramic coatings and the changes produced by moving the cooling passages nearer the trailing edge. This comparison was made to provide a standard for evaluating the gains obtainable with ceramic coatings as compared to those obtainable by constructing the turbine blade in such a manner that water passages could be located very near the trailing edge.

The cooling effectiveness of ceramic coatings was found to depend on the ratio of coating thickness to coating thermal conductivity. For metals of low thermal conductivity (15 Btu/(hr)(sq ft) ($^{\circ}$F/ft)), this ratio should be about 0.05 inch/Btu/(hr)(sq ft)($^{\circ}$F/ft) in order to obtain temperature changes in either metal or gas of the order of those produced by moving the nearest cooling passage from a point 0.6 inch to a point 0.365 inch from the trailing edge of an uncoated blade. When metals of high thermal conductivity (such as copper) are used, the temperature changes produced by ceramic coatings (parameter, 0.05) are about five times the changes obtained by moving the cooling passage. No metal or alloy is currently known that combines high thermal conductivity with the

[redacted]

strength characteristics of high-temperature alloys. In order to secure practical results, very low conductivity ceramics will therefore be needed, such as mica (0.3), or porcelains (0.6), or thoria (very low). With such ceramics, many metals and alloys with intermediate thermal conductivities, between 15 and 210 Btu/(hr)(sq ft)($^{\circ}$F/ft), might become available for turbine use if they are not too weak initially.

INTRODUCTION

Under current aircraft operating conditions, the power and efficiency of gas-turbine engines are limited by the maximum permissible temperature of the combustion gas that can be admitted to the turbine. Several methods of increasing the permissible gas temperature have been suggested: (1) improvement of the blade material to withstand higher temperatures, and (2) cooling of existing material. Both these methods are being investigated at the NACA Cleveland laboratory, but the cooling of existing blade metals is apparently the most expedient means of obtaining higher inlet-gas temperatures. Several methods of cooling turbine blades have been analyzed in references 1 to 10.

In reference 6, the temperature distribution in one type of water-cooled blade is computed. It is shown that the trailing edge of the blade is likely to be the hottest part and that it can be cooled by placing a water passage in the trailing section. For example, in one case the computed trailing-edge temperature was 1782° F when the nearest water passage was 0.6 inch away. Moving this passage to a point 0.25 inch from the trailing edge reduced the trailing-edge temperature to 1300° F. Usually this solution is impractical because the trailing section of the blade is so narrow it will not accommodate a water passage. Another possible solution is to insulate the trailing section by coating it with some low heat-conductivity material, such as a ceramic.

The effect on blade-metal and gas temperatures of adding such coatings to the blade metal with the water passage located far from the trailing edge has been studied at the Cleveland laboratory and is reported herein. A comparison is made between these temperature changes and similar temperature changes of uncoated blades obtained by assuming a water passage nearer the trailing edge. These calculations were made in order to determine relative merits of ceramic coatings compared to water passages near the trailing edge.

The analysis is confined to the trailing section of the blade because that is the part that is usually the most difficult to cool.

For most of the calculations, a representative spanwise line 0.182 inch from the trailing edge is used, that is, halfway between the trailing edge and the nearest cooling passage. The decrease in blade-metal temperature due to the application of various ceramic coatings is first calculated. The coatings range in thickness from 0 to 0.015 inch and in thermal conductivity from 0.25 to 2.50 Btu/(hr)(sq ft)($^{\circ}$F/ft). The two metal thermal conductivities used are 15 and 210 Btu/(hr)(sq ft)($^{\circ}$F/ft). The effective gas temperatures used with these metal conductivities are 1580° and 3270° F, respectively, because they are the largest values the uncoated blade with the water passage 0.6 inch from the trailing edge can withstand without failure for 1000 hours at a tip speed of 1100 feet per second. The gas temperatures are then increased until the critical stress conditions for failure are again reached. This procedure amounts essentially to restoring in the coated blades the same temperatures that prevailed in the uncoated blades. Finally, the last cooling passage is moved from a point 0.6 inch to a point 0.365 inch in front of the trailing edge. The decrease in metal temperature with the same gas temperature is computed as well as the increase in gas temperature required to restore the metal temperature that existed before the cooling passages were moved.

SYMBOLS

The following symbols are used in this analysis:

b height of trapezoid that approximates trailing edge (fig. 1), (ft)

b' $b + \frac{t_{m,t}}{2}$, (ft)

C $\sqrt{U/(k_m \sin \alpha)}$, $(\mathrm{ft})^{-1/2}$

H_0 Hankel function, zero order

H_1 Hankel function, first order

h_o surface heat-transfer coefficient between hot gas and outside blade surface, Btu/(hr)(sq ft)($^{\circ}$F)

h_i surface heat-transfer coefficient between metal and coolant, Btu/(hr)(sq ft)($^{\circ}$F)

J_0 Bessel function of first kind, zero order

J_1 Bessel function of first kind, first order

K constant of proportionality in equation (6)

k thermal conductivity, Btu/(hr)(sq ft)($^{\circ}$F/ft)

L blade span from root to tip, (ft)

T temperature, $^{\circ}$F

T_e effective gas temperature

t thickness (fig. 1), (ft)

U over-all heat-transfer coefficient, $\frac{1}{U} = \frac{1}{h_o} + \frac{t_c}{k_c}$, Btu/(hr)(sq ft)($^{\circ}$F)

x distance from blade root to blade element dx, (fig. 1), (ft)

y distance from blade trailing edge to blade element dy, (fig. 1), (ft)

y' $y + \frac{t_{m,t}}{2}$, (ft)

α one-half angle between sides of trapezoidal approximation for trailing edge, $\alpha = \tan^{-1}\left(\frac{t_{m,b} - t_{m,t}}{2b}\right)$

θ $T_e - T_m$, $^{\circ}$F

μ $2C\left[y' + t_{m,t}\left(\frac{1 - \tan \alpha}{2 \tan \alpha}\right)\right]^{1/2}$

μ_b $2C\left[b' + t_{m,t}\frac{(1 - \tan \alpha)}{2 \tan \alpha}\right]^{1/2}$

μ_t $2C\left[\frac{t_{m,t}(1 - \tan \alpha)}{2 \tan \alpha}\right]^{1/2}$

Subscripts:

b base of trapezoid (fig. 1)

c ceramic

l liquid coolant

m metal

t trailing edge of trapezoid (fig. 1)

ANALYSIS

In the following analysis, the assumptions on which the analysis is based are first given. The equations and methods for getting chordwise and spanwise temperature distributions in the trailing section of the blade for various conditions for either ceramic-coated or uncoated blades are then presented. Finally, methods are given for determining the increase in effective gas temperature when coatings are applied to blades and when water passages are moved closer to the trailing edge. The blade considered and the assumed trapezoidal shape for the trailing portion of the blade are shown in figure 1.

Assumptions

In order to simplify the analysis, the following seven assumptions were made. The assumptions are first listed together and then each one is discussed and separately justified in detail.

(1) The quantity of heat transferred per unit time between the blade surfaces and the heating and cooling fluids is proportional to the temperature difference between the fluid and the blade.

(2) The rate of heat transfer from the hot gas to the blade surface per unit time per unit surface per unit temperature difference is constant over the trailing part of the blade surface.

(3) The temperature at a given point is independent of operating time.

(4) The temperature across the blade thickness is essentially constant.

(5) The heat transfer into the exposed trailing edge can be accounted for by assuming the width extended by a distance equal to one-half the blade thickness at the outer edge and no heat loss from the end.

(6) The actual section with curved sides can be approximated by a trapezoidal section with straight sides.

(7) The effect of heat conduction from a blade section to the turbine rim is negligible for the outer sections of the blade.

Assumption (1) has been shown to be true if the effective temperature (the temperature that the blade will assume when there is no heat transfer) of the fluid is used instead of the stream temperature (references 11 and 12).

Assumption (2) is only approximately true. Theoretical calculations by a number of methods (reference 13) show that variations from the mean of this quantity over the last third of the airfoil section range from 3 to 5 percent according to the method of calculation used when a turbulent boundary layer is assumed. If a laminar layer is assumed, the variation is even less.

As the turbine blades rotate past the nozzle blades, high-frequency changes in the flow into the turbine passages would be expected. Heat conduction is quite a slow process, so such changes would be rapidly damped and the metal temperatures, especially those inside the metal, would attain steady-state temperatures, as postulated in assumption (3).

The relaxation calculations given in reference 6 indicate that assumption (4) is correct except near a curved water passage (fig. 2).

Assumption (5) is discussed at some length in references 4 and 14. In reference 14, it is shown that the fin effectiveness is correct to within 0.1 percent with this assumption. In reference 4, the exact calculation for a blade of uniform thickness shows that in the case in which the error is the largest (high-temperature alloy), the assumption is in error by not more than 0.5 percent. With other metals and a tapered blade, the error will be less.

Assumption (6) was compared with the results of a relaxation calculation in reference 6 and found to agree within approximately $\pm 2^{\circ}$ F.

On the basis of the results of the three-dimensional calculations in reference 4, assumption (7) was made. It is shown in reference 4 that the assumption is true for blade sections more than 1 inch from the rim for a metal conductivity of 15 Btu/(hr)(sq ft)($^{\circ}$F/ft) and for sections more than 3 inches from the rim for a metal conductivity of 210 Btu/(hr)(sq ft)($^{\circ}$F/ft). For the second part of this report, which deals with possible increases in effective gas temperature, this assumption is modified.

Blade-Metal Temperatures

The distribution of blade-metal temperatures is needed in two directions, chordwise (perpendicular to the water passage and the trailing edge) and spanwise (parallel to the water passage).

<u>Chordwise temperature distribution.</u> - In the case of a trapezoidal section (fig. 1) with hot gas on three sides and water flowing on the wide base, the following temperature equation is developed in reference 4:

$$T_e - T_m = \theta = \frac{\frac{h_i\mu_b}{2C^2k_m}(T_e - T_l)\left[H_1(i\mu_t)J_0(i\mu) + iJ_1(i\mu_t)iH_0(i\mu)\right]}{\left[iJ_1(i\mu_t)H_1(i\mu_b)\right] - \left[H_1(i\mu_t)iJ_1(i\mu_b)\right] + \frac{h_i\mu_b}{2C^2k_m}\left[H_1(i\mu_t)J_0(i\mu_b) + iJ_1(i\mu_t)iH_0(i\mu_b)\right]} \tag{1}$$

where

i $\quad\sqrt{-1}$

μ $\quad 2C\left[y' + t_{m,t}\left(\frac{1 - \tan\alpha}{2\tan\alpha}\right)\right]^{1/2}$

μ_b $\quad$ value of μ when $y' = b$, that is, at water passage

μ_t $\quad$ value of μ when $y' = 0$, that is, just beyond trailing edge

If a wedge-shaped section is used,

$$t_{m,t} \doteq 0$$

hence

$$\mu_t \doteq 0$$

Therefore

$$H_1(i\mu_t) \doteq \infty$$

$$iJ_1(i\mu_t) \doteq 0$$

Equation (1) then takes the simpler form,

$$\theta = \frac{\frac{h_i\mu_b}{2C^2k_m}(T_e - T_l)J_0(i\mu)}{\frac{h_i\mu_b}{2C^2k_m}J_0(i\mu_b) - iJ_1(i\mu_b)} \tag{2}$$

When a ceramic coating is applied to the blade, its influence on the blade-temperature distribution is calculated by the method used for scale deposits in boiler work (reference 15, p. 36). In equation (1), the value of C is

$$C = \left(\frac{h_o}{k_m \sin \alpha}\right)^{1/2} \tag{3}$$

When a ceramic coating is interposed between the metal and the hot gas, the over-all heat-transfer coefficient U from hot gas to metal is given by the relation

$$\frac{1}{U} = \frac{1}{h_o} + \frac{t_c}{k_c} \tag{4}$$

If U replaces h_o in equation (3), the new distribution will include the effect of the ceramic and the new value of C will be

$$C = \left(\frac{U}{k_m \sin \alpha}\right)^{1/2} \tag{5}$$

This change is the only one needed if a ceramic coating is added to the blade metal without changing the metal dimensions. If the original blade dimensions are to be retained and metal removed to make room for the ceramic, then the metal dimensions b and $t_{m,t}$ will also be altered.

Spanwise temperature distribution. - Two distributions are calculated in the spanwise direction: an allowable distribution based on the temperature-stress properties of the metal under study, and an actual distribution based on the equations and the curves of reference 4.

In order to find the allowable temperature curve, the criterion of blade failure is assumed to be longitudinal stress rupture in tension. The value of the stress at which this rupture occurs is found by experiment and for a given material depends on the time and the temperature (reference 16). The data presented in reference 16 for cast S816 blade metal were used as representing a reasonable sample of high-temperature alloy. A reasonable life was assumed to be 1000 hours. With these assumptions, the maximum allowable temperature at any point on the blade depends only on the stress at that point, which in turn depends on the radial distance from the axis of rotation and the rotational speed. The tip speed in the present report is assumed to be 1100 feet per second. The maximum allowable temperature therefore becomes a single-valued function of the radial distance from the rotation axis. The allowable-temperature curve found in this way is plotted in figure 3 as a function of the position on the blade of the point in question (expressed here as the ratio of the distance from blade root to the blade span x/L).

The actual temperature distribution spanwise is calculated for a line parallel to the water passage and the trailing edge through point E (fig. 1) near the rear of the trailing section. Along this path, a typical spanwise temperature distribution for an uncoated blade is shown in curve A of figure 3. This curve, taken from reference 4, was worked out by a Fourier series calculation for a blade section of uniform thickness for a given set of conditions. It is assumed that the curve will have essentially the same shape for a blade section of variable thickness.

When a ceramic coating is applied to the blade, the temperature of the flat portion of the curve can be calculated from equations (1), (4), and (5) and will be somewhat lower as shown in curve B (fig. 3). If the assumption is made that the addition of the ceramic coating does not appreciably affect the temperature of the turbine rim (blade root), then a simple proportion may be written for the temperature relations between the two curves.

$$T_{m,B} - T_{m,r} = K(T_{m,A} - T_{m,r}) \tag{6}$$

where

$T_{m,A}$ temperature given by curve A

$T_{m,B}$ temperature given by curve B for same abscissa

$T_{m,r}$ temperature of blade root

The constant of proportionality K can easily be found for the flat portion of the curves and is assumed to hold for the curved portions also.

Effect of Ceramic Coatings on Blade Temperature Drop

In order to find the effect of ceramic coatings on the blade temperature drop, the temperatures of the blade metal (no ceramic coating) were calculated from equation (1). Then ceramic coatings were applied and new blade-metal temperatures were calculated from equations (1), (4), and (5). The difference between the old and new temperatures at any given point (usually E) gave the blade temperature drop.

Effect of Ceramic Coatings on Increase of Effective Gas Temperature

When curves A and B and the curve of allowable temperature have been found, as illustrated in figure 3 and previously explained, the permissible values of effective gas temperature can be found. This result is accomplished by adjusting the effective gas temperatures in curves A and B so as to cause both curves, first A and then B, to become tangent to the allowable temperature curve.

Inspection of equation (1) shows that the ratio $\dfrac{T_e - T_m}{T_e - T_l}$ depends only on other physical constants such as h_i, h_o, k_m, and so forth. Accordingly, if the mean water temperature T_l is assumed to remain constant while T_e is changed to another value T_e', then the new metal temperature T_m' will be given by the simple proportion

$$\frac{T_e' - T_m'}{T_e' - T_l} = \frac{T_e - T_m}{T_e - T_l} \tag{7}$$

By adjusting T_e' by trial, the actual-temperature curve A is moved to a new position C tangent to the allowable temperature curve (fig. 3). Then in the same manner, B is moved to become tangent to the allowable-temperature curve by changing T_e to some value T_e''. The permissible increase in effective gas temperature is the difference between these two temperatures $T_e'' - T_e'$.

APPLICATION OF ANALYSIS

The following values were used in all calculations to be presented:

Gas-flow rate, lb/sec 55
Average hot-gas-to-blade heat-transfer coefficient,
h_o, Btu/(hr)(°F)(sq ft) 217
Coolant-water-flow rate, lb/min/blade 7
Average metal-to-coolant heat-transfer coefficient, h_i,
Btu/(hr)(°F)(sq ft)
Two-hole blade (fig. 1) 2370
Five-hole blade (fig. 4) 2134
Gas temperature used for uncoated, two-hole blade calculations when metal was assumed to be S816 (thermal conductivity, 15 Btu/(hr)(°F)(sq ft)), °F 1580
Gas temperature used for uncoated, two-hole blade calculations when metal was assumed to be S816 (thermal conductivity, 210 Btu/(hr)(°F)(sq ft)), °F 3270

The gas flow rate used in the calculations is the design value for the turbine with the blade shape used in this report. The estimate of the gas-to-metal heat-transfer coefficient using the blade dimensions shown in figure 4 was made using data from the General Electric Company. In this data, the values of the Reynolds number and the Nusselt number are computed by using the blade perimeter divided by π for the hydraulic diameter and by evaluating the viscosity and conductivity of the fluid at the arithmetic mean temperature between the metal and the gas. In reference 8, a similar method of estimating the outside blade heat-transfer coefficient is presented. When this method is applied to the present conditions, a value of about 220 Btu/(hr)(sq ft)(°F) is obtained for the blade surface heat-transfer coefficient. This value agrees closely with the value used in this report and also with another value calculated using data from reference 15 (p. 236). The average metal-to-coolant heat-transfer coefficients were obtained using the dimensions of the water passages shown in figure 4. The correlation equation ((4C), reference 15, p. 168) was used for the

calculation. The water thermal conductivity, specific heat, and viscosity were evaluated at a water bulk temperature of 200° F. The calculated values of h_o and h_i agreed fairly well with those that were consistent for temperatures obtained in the Schmidt water-cooled turbine (from a report by the U. S. Strategic Air Forces in Europe). The gas temperatures used in the calculations of the two-hole uncoated blade temperatures were the largest values allowed by the permissible increase in gas-temperature calculations. The metal-strength characteristics used in the calculations with high-conductivity metal were assumed to be the same as those actually available for high-temperature, low-conductivity alloys such as S816. Such a material of high conductivity and strength characteristics of S816 is, of course, not currently available.

Calculations of the decreases in blade-metal temperatures and increases in effective gas temperatures when ceramic coatings of various thicknesses and conductivities are placed on the surface of the two-hole blade of figure 4 were made. Calculations showed that it was more advantageous to place the ceramic on the original blade configuration rather than cut the metal back and retain the original outside dimensions after the ceramic coating is placed on the metal surface. Point E of figure 1 was the position at which these effects were investigated. The assumed conditions that were used for these calculations for figures 5 to 7 are summarized in the following table:

Figure	k_m (Btu/(hr)(sq ft)(°F/ft))	k_c (Btu/(hr)(sq ft)(°F/ft))	t_c (in.)	T_e (°F)	T_l (°F)
5	15	Uncoated	Uncoated	1580	200
	210			3270	200
6	15	0.25 to 2.50	0-0.015	1580	200
	210	.25 to 2.50	0- .015	3270	200
7	15	0.25 to 2.50	0-0.015	Variable	200
	210	.25 to 2.50	0- .015	Variable	200

The value 0.25 Btu/(hr)(sq ft)(°F/ft) for the ceramic conductivity corresponds to that of the best solid heat insulators such as mica. The value 2.50 Btu/(hr)(sq ft)(°F/ft) corresponds to the common magnesium-oxide type of ceramic material (reference 17).

Calculations were also made of the decrease in metal temperature at point E (fig. 1) and the increase in effective gas temperature, with the spanwise distribution at position E determining allowable gas temperatures when the five holes (fig. 4) were used in the uncoated blade rather than the two holes. Equations (1) and (3) and the methods given in the analysis were used to determine these temperature changes. Calculations of blade-metal temperature distribution along axis O-A (fig. 1) from the trailing edge to a distance of 0.365 inch from the trailing edge and near the blade tips for both the five-hole and two-hole blades were also made. These calculations were primarily made to determine whether point E was a position that would give representative values of that increase when used in the determination of increase in effective gas temperature. The points between E and the trailing edge had nearly the same temperature drop as E and the permissible increase in gas temperature was not very different. In these calculations for the uncoated blades, the metal conductivities, effective gas temperatures, and water temperatures used were the same as those listed in the foregoing table.

RESULTS AND DISCUSSION

The isothermal lines across the cross section of the two-hole uncoated blade for a metal thermal conductivity of 15 Btu/(hr)(sq ft)($^{\circ}$F/ft) and an effective gas temperature of 1580° F are shown in figure 2. These temperatures are applicable spanwise to all points more than 1 inch from the blade root. These data were obtained from the work sheets used in reference 6 by converting the effective gas temperature from 2000° (used in reference 6) to 1580° F. Equation (7) was used in making the conversion. The fact that the isothermal lines are nearly straight across most of the trailing section shows that assumption (4) is a good approximation. It is at once evident that the leading and trailing edges are the hottest places on such a blade. In an actual case, the effective gas temperature and the heat-transfer coefficient would be largest at the leading edge and would decrease toward the trailing edge. Thus the leading-edge temperature would be higher than shown and the trailing edge less, but not enough to make any substantial difference in the general values, that is, the trailing edge would still be the hottest region and the leading edge the next hottest.

The five-hole blade (fig. 4), provides a cooling passage 0.365 inch from the trailing edge and the two-hole blade provides one 0.600 inch from the trailing edge. The results of the calculations of metal temperatures from the trailing edge to

0.365 inch from the trailing edge for these two blade configurations are shown in figure 5. The effective gas temperatures and metal conductivities for which the calculations were made are noted on the curves. The curves show that when the metal conductivity k_m is 15 Btu/(hr)(sq ft)($^{\circ}$F/ft) and the effective gas temperature T_e is 1580° F, the average metal temperatures for the five-hole blade are reduced about 250° F below those for the two-hole blade; whereas when k_m is 210 Btu/(sq ft)(hr)($^{\circ}$F/ft) and T_e is 3270° F, the metal temperature reduction is about 90° F. This cooling is uniform throughout the trailing section for the high-conductivity material, whereas for the low-conductivity material, it varies from about 400° F at the cooling passage to 130° F at the trailing edge. The high conductivity would be expected to equalize the cooling effect throughout the material.

The difference in the shape of the temperature-distribution curves in the two cases (reference 4) causes the metal temperatures to be higher for the high-conductivity metal. It is evident in reference 4, as mentioned in the discussion of assumption (7), that with low-conductivity metal the curve of temperature distribution flattens at an x/L value of about 25 percent and with high-conductivity metal at about 75 percent so that in figure 3 the point of contact of the allowable and actual blade-temperature curves occurs for the high-conductivity metal at a considerably larger value of x/L than for the low-conductivity metal. The allowable metal temperature at this point is higher for the larger x/L value because the metal stresses are smaller. In different words, the rim-cooling effect is larger for the high-conductivity metal than for the low-conductivity metal. As pointed out in APPLICATION OF ANALYSIS, the metal of high conductivity for turbine blades is unavailable and the results of the analysis using this metal (fig. 5 and following fig. 3) are tentative.

The differences between metal temperatures at point E of the uncoated and ceramic-coated two-hole blade are plotted in figure 6 against the ratio of ceramic thickness to ceramic conductivity t_c/k_c. The differences are noted as decreases in temperature, which is the decrease in temperature of the coated blade as compared to the uncoated-blade temperature. The use of the parameter t_c/k_c enables all the different ceramic types to be plotted on a single curve. It shows also that a decrease in thermal conductivity of the ceramic has the same effect as an increase in coating thickness and that if thickness is to be small for a given amount of cooling, then the ceramic conductivity must also be small. The curve for the lower effective gas temperature, 1580° F, shows cooling at point E up to 250° F whereas the curve for the higher gas

temperature (3270° F) and metal conductivity (210 Btu/(hr)(sq ft)(°F/ft)) shows decreases up to about 490° F. This result compares with decreases of 210° and 90° F, respectively, produced by moving the cooling passage nearer the trailing edge as shown by the symbols on the ordinate at a t_c/k_c of 0. The results showed that when a low metal conductivity is used for ceramic coatings of practical thicknesses, the very lowest ceramic conductivity (about 0.25) must be used to obtain trailing-edge temperatures comparable to those obtained when the water passage is moved close to the trailing edge. For high metal conductivities, however, much lower trailing-edge temperatures, by about 400° F, can be obtained with ceramic coatings of low conductivity and practical thicknesses than by using water passages very close to the trailing edge. The difference between the two curves of figure 6 is due almost entirely to the difference in effective gas temperatures. If the upper curve had been calculated for an effective gas temperature of 1580° F but with a thermal conductivity of 210 Btu/(hr)(sq ft)(°F/ft), then it would have been quite near the lower curve (within 25° F when $t_c/k_c = 0.06$).

The permissible increases in the effective gas temperatures as a function of the same ceramic parameter t_c/k_c for the same conditions as those of figure 6 are shown in figure 7. For the low metal conductivity, these increases approach a value of 400° F; for the high metal conductivity, the maximum effective gas temperature increase for the range of t_c/k_c studied is almost equal to 2100° F. The results on the effect of the ceramic coatings compared with the results on the effect of placing a water passage much closer to the trailing edge in figure 7 are very similar to those of figure 6. That is, when a low-conductivity metal is used for ceramic coatings of practical thickness (not exceeding 0.015 in.), very low-conductivity ceramics must be used in order to obtain increases in effective gas temperature comparable with those obtained by moving the water passage closer to the trailing edge. Thus, in figure 7, a value of t_c/k_c of about 0.045 is required to obtain an increase comparable to that shown by the circle on the ordinate line (about 325° F). If t_c were 0.010 inch, then k_c would have to be 0.22 Btu/(hr)(sq ft)(°F/ft) (a very low conductivity) in order to get this gas temperature increase. For the high-conductivity metal, however, in most cases much greater increases, (about five times) in effective gas temperatures are shown in figure 7 when ceramic coatings are used than when the water passage is moved closer to the trailing edge. The increase for the high-conductivity metal indicated by the triangle on the ordinate line, is about 275° F. This value is exceeded for all values of t_c/k_c greater than 0.007.

It is evident that the application of ceramic coatings produces the greatest effect on either the blade metal or the effective gas temperature when the metal combines a high thermal conductivity with good strength at metal temperatures of 1200° to 1400° F. No metal nor alloy is in current use that provides this combination. The high-strength metals have low thermal conductivities whereas the high-conductivity metals are weak at high temperatures.

If the blades are made of high-temperature alloy, very low ceramic conductivities will be needed to produce temperature changes comparable with those attainable by moving the cooling-water passages nearer the trailing edge. Mica at 100° F has a thermal conductivity of less than 0.3 Btu/(hr)(sq ft)(°F/ft) and if it could be used for such coatings would require only a thickness of 0.015 inch to produce an increase in gas temperature of 300° F. Thoria may have a thermal conductivity of this same order but conductivity measurements will be required to find out. Porcelains and some other ceramics are available with thermal conductivities of about 0.5 to 0.6 Btu/(hr)(sq ft)(°F/ft). These materials could produce moderate temperature increases especially if greater coating thicknesses could be used. A large number of metals and alloys, such as beryllium-copper, and bronze, exist that have thermal conductivities between 15 and 210 Btu/(hr)(sq ft)(°F/ft) and hence would give intermediate values of temperature change (between 300° and 1000° F) if they are not too weak. Ceramic coatings should also be quite effective in the case of aluminum blades. Much experimental work must be done on the application of ceramic coatings to blades to determine physical and heat-transfer properties.

SUMMARY OF RESULTS

From an analysis of the effect of ceramic coatings on water-cooled turbine blades, the following results were obtained:

1. The cooling effectiveness of ceramic coatings depended on the ratio of the thickness of the coating to the thermal conductivity of the coating.

2. For practical coating thicknesses in the case where the metal conductivity was low (15 Btu/(hr)(sq ft)(°F/ft)), up to a thickness of about 0.015 inch, ceramic-coating conductivities had to be very low (about 0.25 Btu/(hr)(sq ft)(°F/ft)) to obtain appreciable decreases in blade-metal temperatures or increases in effective gas temperatures as compared to temperatures obtained with no coating.

3. In order to obtain decreases in blade-metal trailing-edge temperatures or increases in effective gas temperatures of the order of those obtained when the cooling passage was moved from a point 0.6 inch to a point 0.365 inch from the trailing edge of an uncoated high-temperature alloy blade, ceramic coatings with a ratio of thickness to thermal conductivity equal to about 0.05 had to be applied to the blade whose cooling passage is 0.6 inch from the trailing edge.

4. When the metal conductivity was very high, about equal to that of copper, ceramic coatings with a ratio of thickness to thermal conductivity of only 0.007 produced the same temperature changes, either gas or metal, that moving the cooling passage from 0.6 to 0.365 inch from the trailing edge produced. Ceramic coatings with a ratio of thickness to thermal conductivity equal to or greater than 0.05 produced about five times the temperature changes that were obtained by moving the cooling passage.

5. Results showed that in order to secure practical results, very low conductivity ceramics will be needed, such as mica (0.3), or porcelains (0.6), or thoria (very low). With such ceramics, many metals and alloys with intermediate thermal conductivities, between 15 and 210 Btu/(hr)(sq ft)($^{\circ}$F/ft), might become available for turbine use if they are not too weak initially.

Lewis Flight Propulsion Laboratory,
National Advisory Committee for Aeronautics,
Cleveland, Ohio.

REFERENCES

1. Brown, W. Byron: Cooling of Gas Turbines. I - Effects of Addition of Fins to Blade Tips and Rotor, Admission of Cooling Air through Part of Nozzles, and Change in Thermal Conductivity of Turbine Components. NACA RM No. E7B11a, 1947.

2. Wolfenstein, Lincoln, Meyer, Gene L., and McCarthy, John S.: Cooling of Gas Turbines. II - Effectiveness of Rim Cooling of Blades. NACA RM No. E7B11b, 1947.

3. Brown, W. Byron, and Livingood, John N. B.: Cooling of Gas Turbines. III - Analysis of Rotor and Blade Temperatures in Liquid-Cooled Gas Turbines. NACA RM No. E7B11c, 1947.

4. Brown, W. Byron, and Monroe, William R.: Cooling of Gas Turbines. IV - Calculated Temperature Distribution in the Trailing Part of a Turbine Blade Using Direct Liquid Cooling. NACA RM No. E7B11d, 1947.

5. Wolfenstein, Lincoln, Maxwell, Robert L., and McCarthy, John S.: Cooling of Gas Turbines. V - Effectiveness of Air Cooling of Hollow Blades. NACA RM No. E7B11e, 1947.

6. Livingood, John N. B., and Sams, Eldon W.: Cooling of Gas Turbines. VI - Computed Temperature Distribution through Cross Section of Water-Cooled Turbine Blade. NACA RM No. E7B11f, 1947.

7. Sanders, J. C., and Mendelson, Alexander: Theoretical Evaluation of Methods of Cooling the Blades of Gas Turbines. NACA RM No. E7B11g, 1947.

8. Reuter, J. George, and Gazley, Carl, Jr.: Computed Temperature Distribution and Cooling of Solid Gas-Turbine Blades. NACA RM No. E7B11h, 1947.

9. Bressman, Joseph R., and Livingood, John N. B.: Cooling of Gas Turbines. VII - Effectiveness of Air Cooling of Hollow Turbine Blades with Inserts. NACA RM No. E7G30, 1947.

10. Brown, W. Byron, and Livingood, John N. B.: Cooling of Gas Turbines. VIII - Theoretical Temperature Distributions through Gas Turbine with Special Blades and Cooling Fins on the Rim. NACA RM No. E7I22a, 1948.

11. McAdams, William H., Nicolai, Lloyd A., and Keenan, Joseph H.: Measurements of Recovery Factors and Coefficients of Heat Transfer in a Tube for Subsonic Flow of Air. NACA TN No. 985, 1945.

12. Eckert, E., and Weise, W.: The Temperature of Unheated Bodies in a High-Speed Gas Stream. NACA TM No. 1000, 1941.

13. Boelter, L. M. K., Grossman, L. M., Martinelli, R. C., and Morrin, E. H.: An Investigation of Aircraft Heaters. XXIX - Comparison of Several Methods of Calculating Heat Losses from Airfoils. NACA TN No. 1453, 1948.

14. Harper, D. R., 3d, and Brown, W. B.: Mathematical Equations for Heat Conduction in the Fins of Air-Cooled Engines. NACA Rep. No. 158, 1922.

15. McAdams, William H.: Heat Transmission. McGraw-Hill Book Co., Inc., 2d ed., 1942, pp. 36, 168, 236.

16. Machlin, E. S., and Nowick, A. S.: Stress Rupture of Heat-Resisting Alloys as a Rate Process. NACA TN No. 1126, 1946.

17. Riddle, Frank H.: Ceramic Insulation for Spark Plugs. S.A.E. Jour. (Trans.), vol. 46, no. 6, June 1940, pp. 236-242.

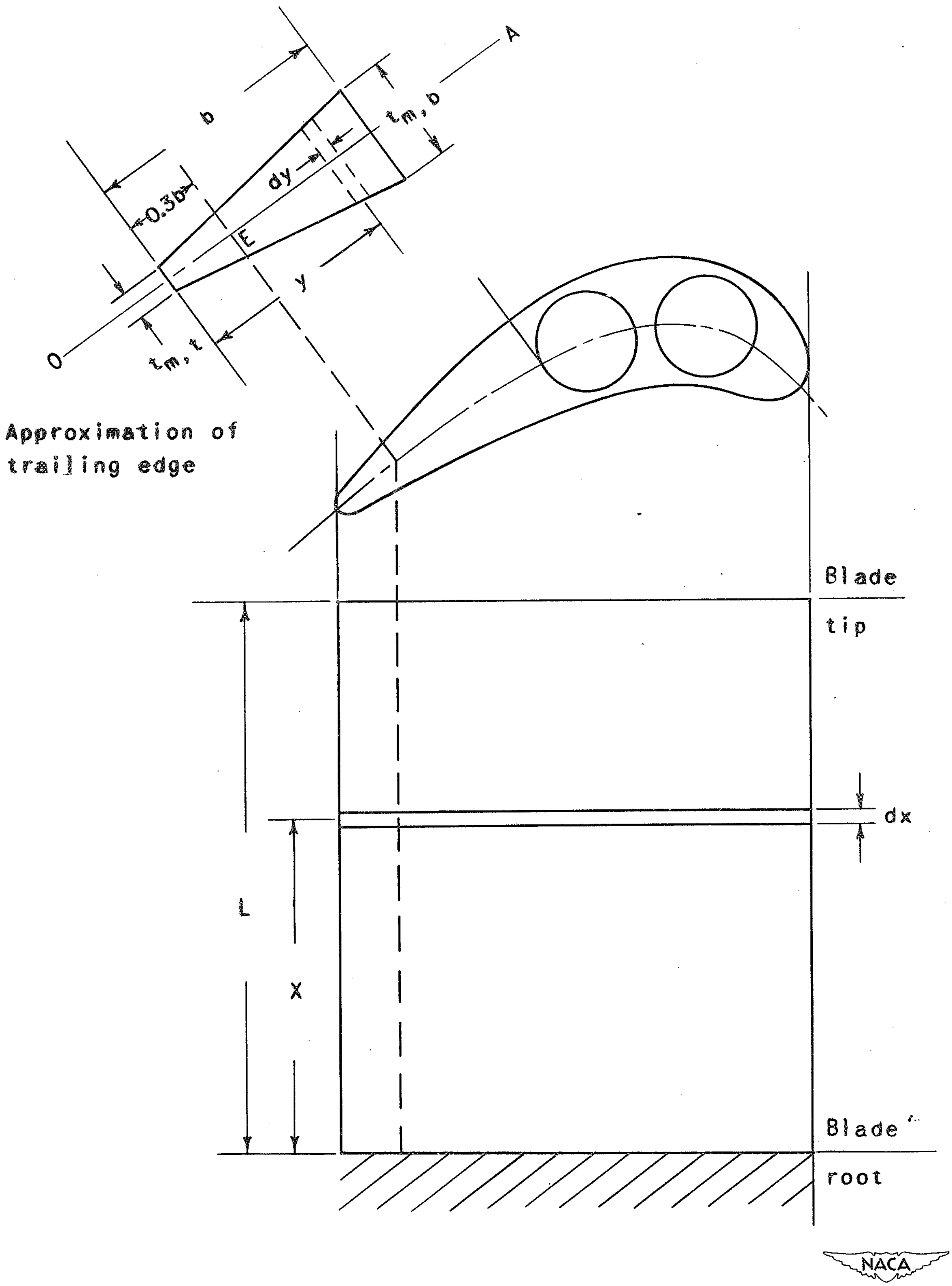

Figure 1. - Notation for liquid-cooled turbine blade. Spanwise temperature distribution made at point E.

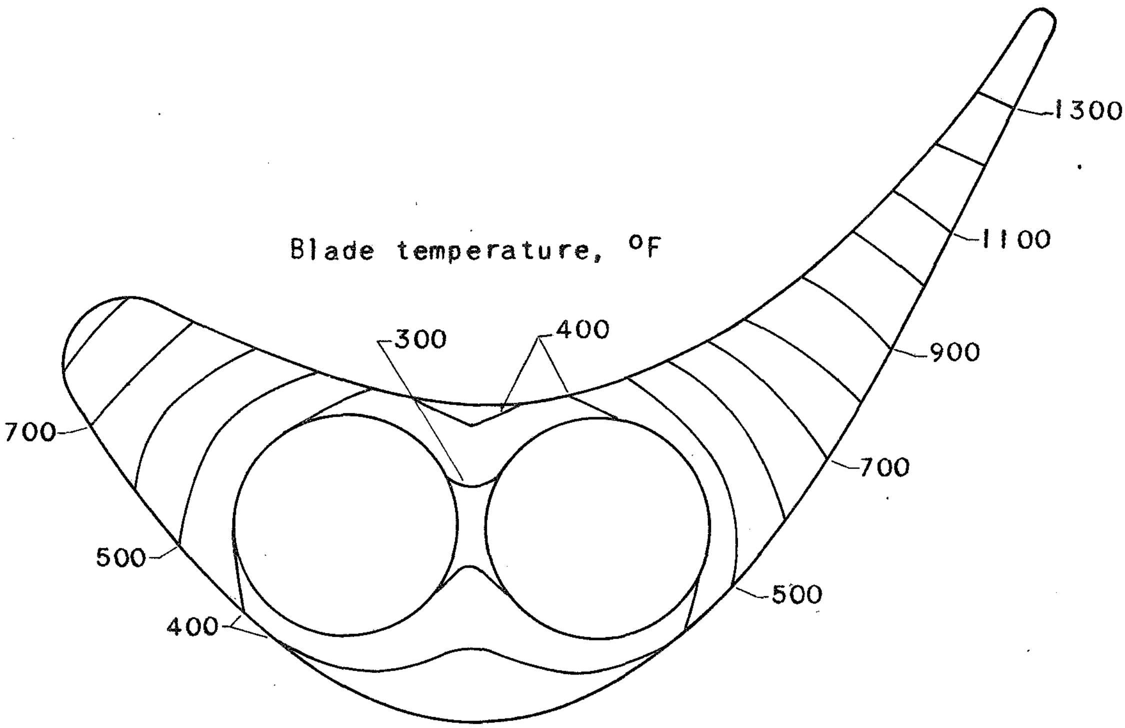

Figure 2. - Temperature distribution through cross section of water-cooled turbine blade. Thermal conductivity of metal, 15 Btu/(hr)(sq ft)(°F/ft); effective gas temperature, 1580° F; average water temperature, 200° F.

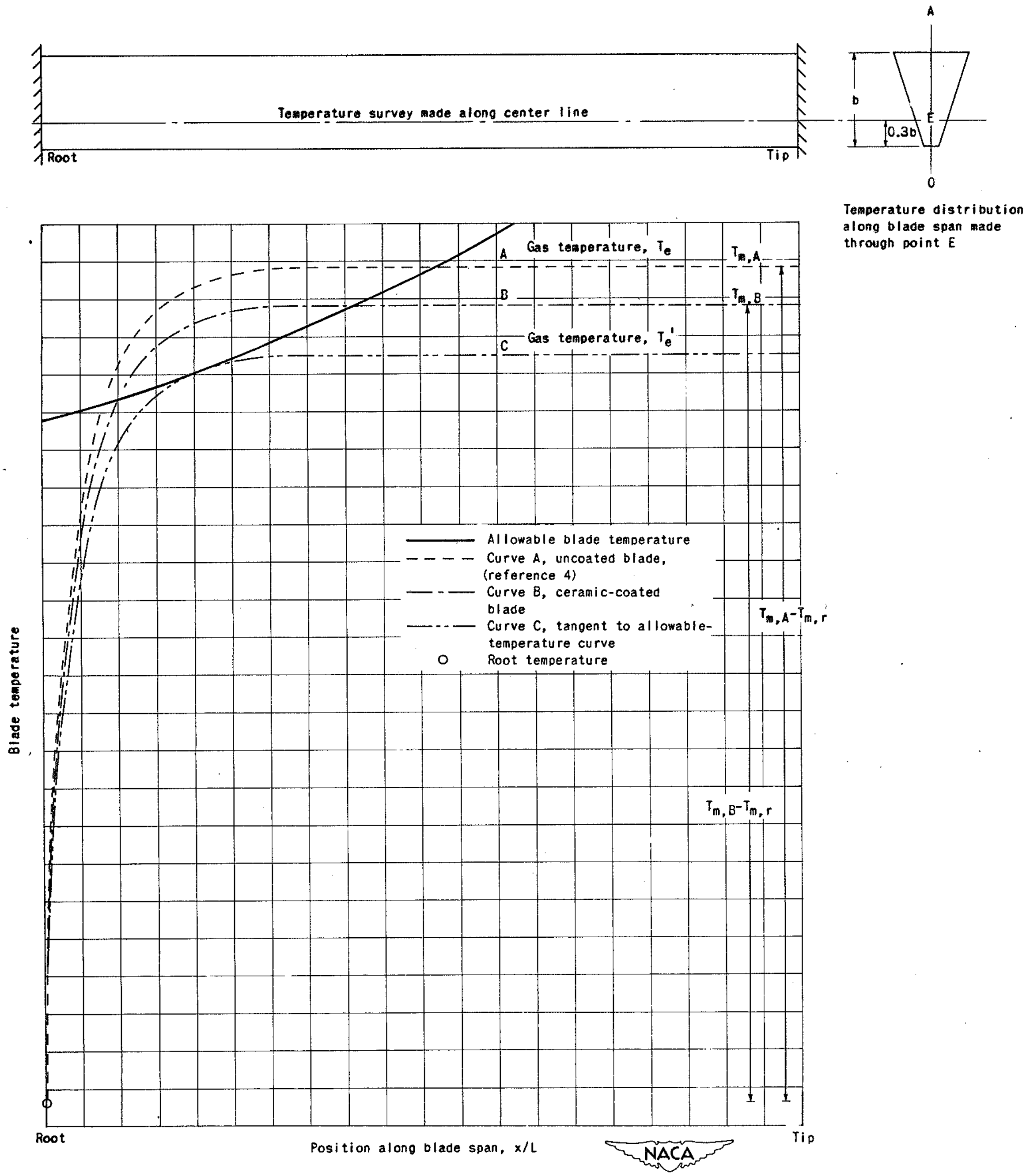

Figure 3. – Spanwise temperature distribution along center of trailing blade section.

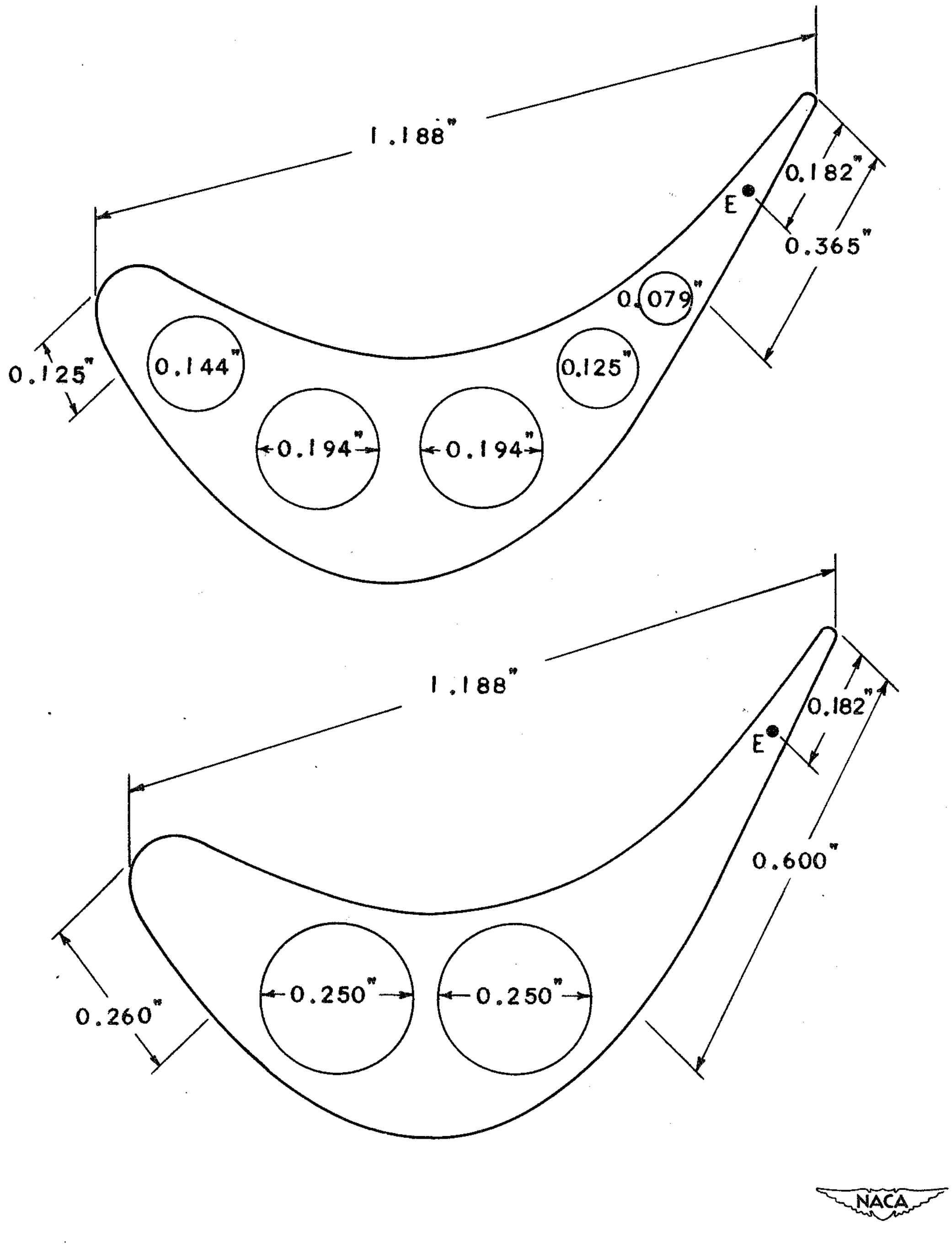

Figure 4. - Cross section of water-cooled turbine blades showing location and size of cooling passages and blade dimensions. Turbine blade dimensions: blade span, 4 inches; perimeter of blade heating surface, 3.05 inches; area of blade, 0.29 square inch.

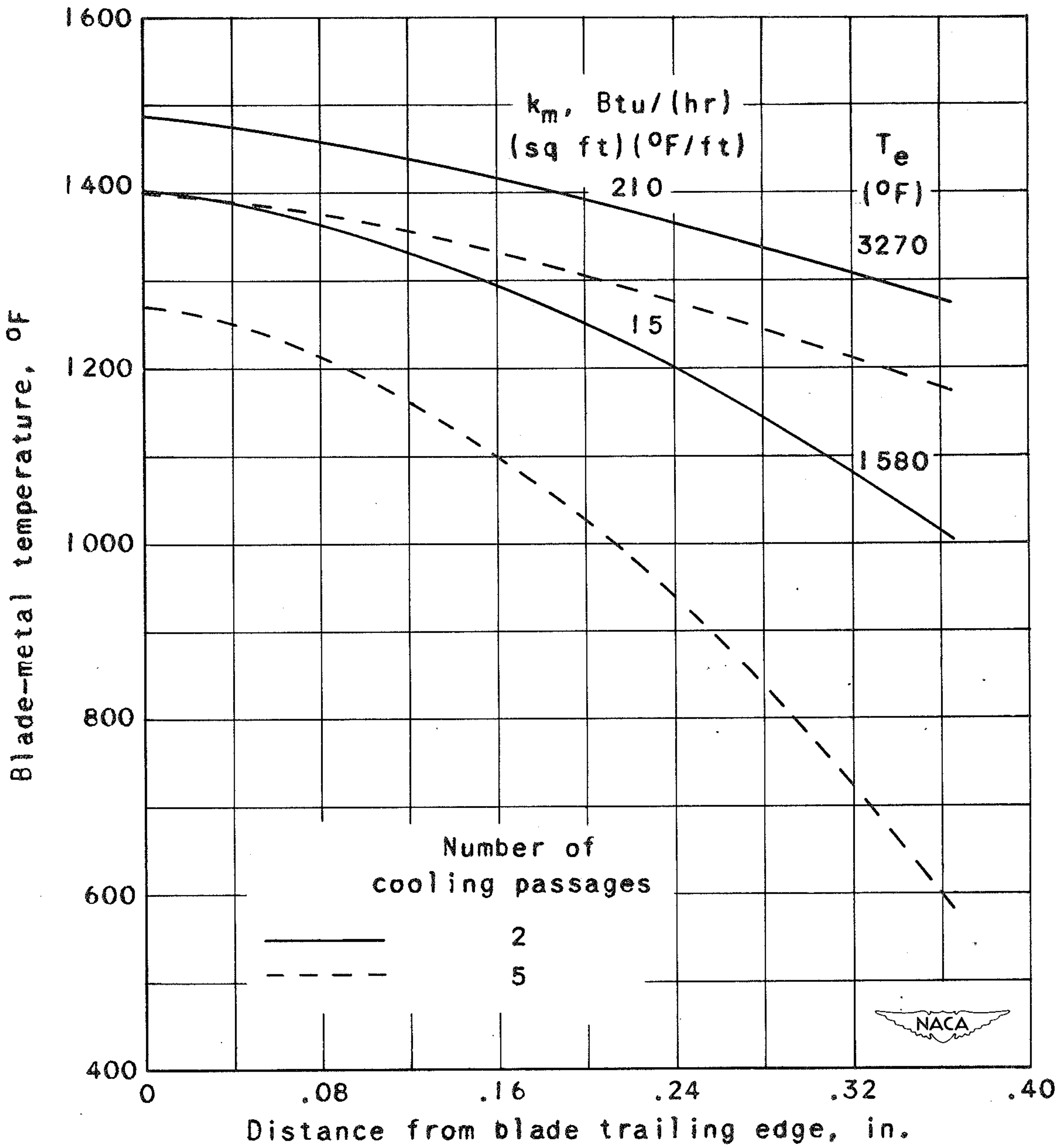

Figure 5. - Comparison of blade-metal temperatures of blades with two and five cooling passages for two values of effective gas temperature and thermal conductivity.

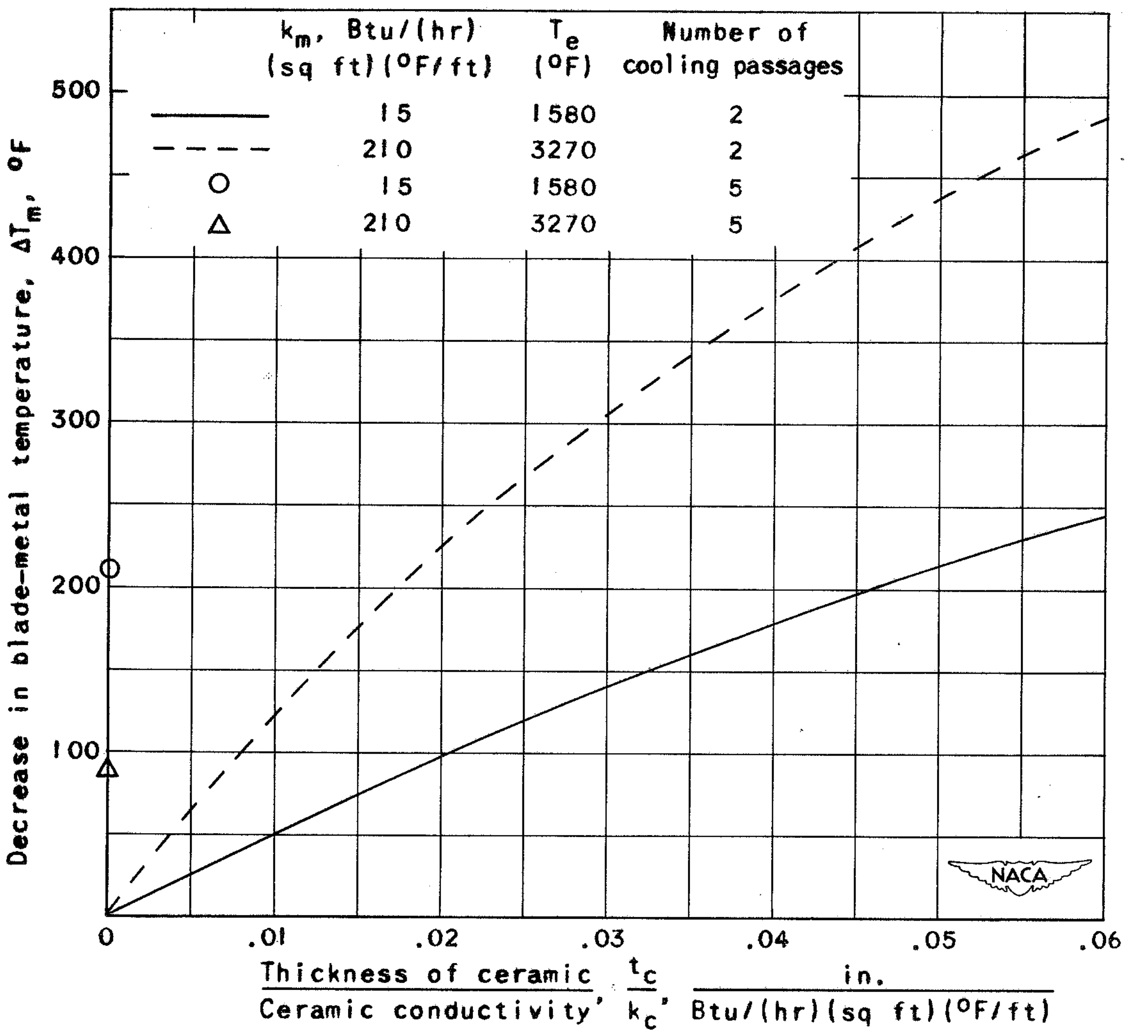

Figure 6. - Effect of ceramic coating on blade-metal temperature. Blade-metal temperature taken 0.182 inch from blade trailing edge.

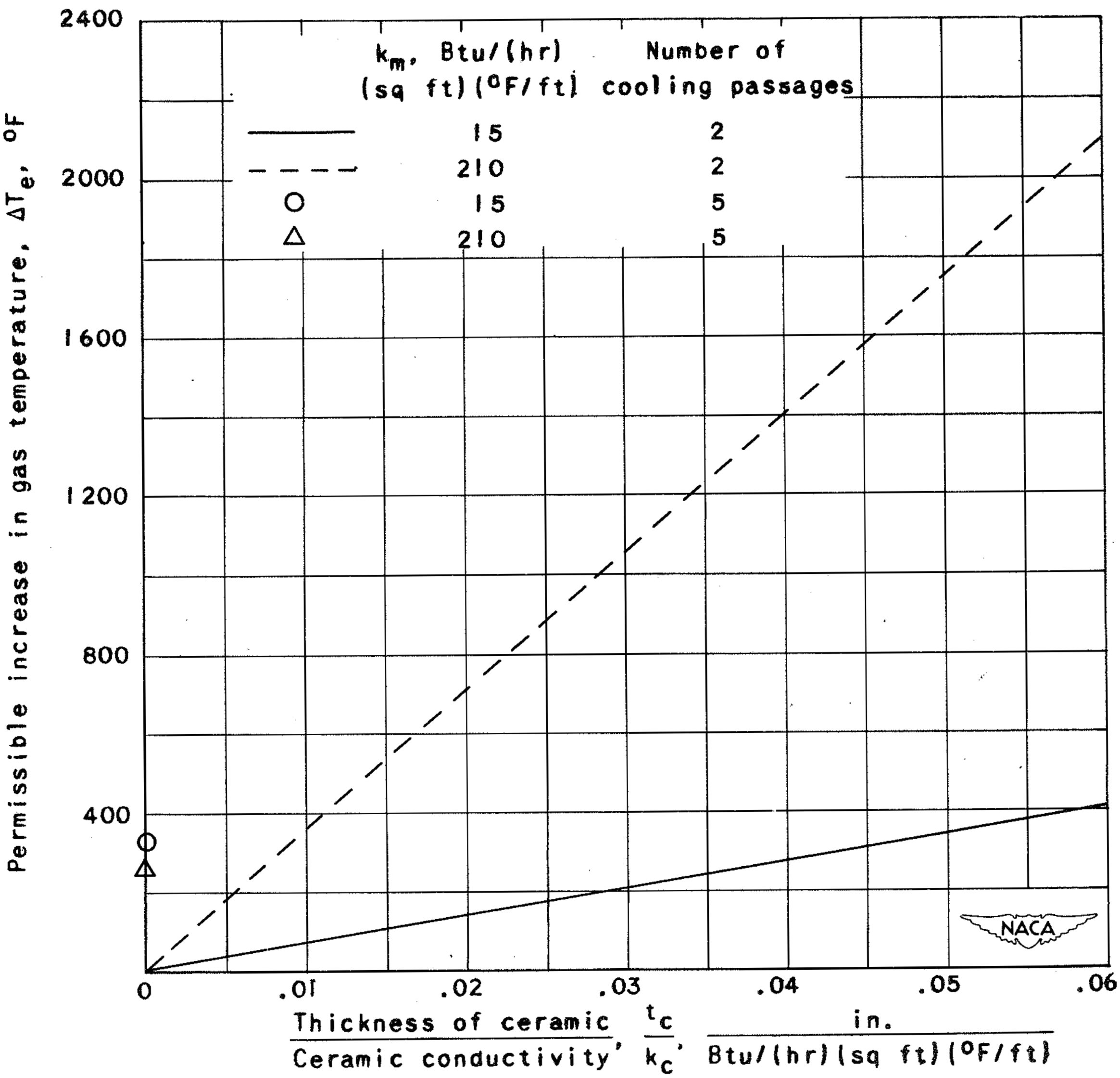

Figure 7. - Effect of ceramic coating on permissible gas temperature. Blade-metal temperature taken 0.182 inch from blade trailing edge.

10-7-71